MINISTRY OF EDUCATION AND TRAINING
MINISTRY OF AGRICULTURE AND RURAL DEVELOPMENT

VIETNAM ACADEMY FOR WATER RESOURCES

MAI TRONG LUAN

STUDY ON WAVE REDUCTION EFFICIENCY OF MODULAR BREAKWATER WITH CT3N-WIP1 COMPONENTS, APPLIED FOR COASTAL PROTECTION IN THE WEST SEA OF CA MAU PROVINCE

SPECIALIZTION: HYDRAULIC CONSTRUCTION ENGINEERING

CODE: 9 58 02 02

SUMMARY OF THESIS OF HYDRAULIC ENGINEERING

Supervisors:

Supervisors 1. Prof.Dr. Nguyen Vu Viet
Supervisors 2. Prof.Dr. Thieu Quang Tuan

Ha Noi - 2024

The thesis was completed at:

Vietnam Academy for Water Resources

Advisor 1. Prof.Dr. Nguyen Vu Viet

Advisor 2. Prof.Dr. Thieu Quang Tuan

Reviewer 1: Assoc. Prof. Dr. Nguyen Ba Quy

Reviewer 2: Assoc. Prof. Dr. Nguyen Viet Thanh

Reviewer 3: Prof. Dr. Le Van Nghi

The thesis will be defended in front of Examination Committee at Vietnam Academy for Water Resources.

Add: No. 171 Tay Son, Dong Da District, Hanoi.

Time: …… hh ……, …… December, 2024

The thesis can be found at:

- The National library

- Library of Vietnam Academy for Water Resources

INTRODUCTION

1. Rationale

Coastal erosion and the degradation of mangrove ecosystems (ME) are pressing issues. In the Mekong Delta region, particularly along the West Sea of Ca Mau province, these problems have become severe challenges, directly impacting the economy, environment, and livelihoods of millions of coastal residents. Current coastal protection solutions include hard engineering structures such as concrete dikes and stone revetments, as well as soft solutions like bamboo fences and mangrove plantation. However, each solution has its limitations. In this context, researching and implementing effective wave reduction measures that ensure sustainability and support the restoration of mangrove ecosystems has become a critical necessity. The CT3N-WIP1 structure—a novel modular, porous, and hollow design—has been proposed as an advanced solution to address these shortcomings.

2. Research objectives

To clarify the correlation between the geometric parameters of the modular porous breakwater constructed with CT3N-WIP1 components and the wave transmission coefficient, and to establish an empirical formula for calculating the wave transmission coefficient (K_t) of these structures.

3. Scope of resesearch

Subjects of Research: The process of wave transmission through modular porous breakwaters constructed with CT3N-WIP1 components under specific hydrodynamic conditions in the West Sea of Ca Mau province.

Scope of Research: Modular porous breakwaters constructed with CT3N-WIP1 components, installed on muddy beaches in front of eroded mangrove belts in the West Sea of Ca Mau province.

4. Content of Implementation

- Overview of related studies.

- Investigation of wave transmission through modular porous breakwaters using physical model experiments.

- Development of an empirical formula to evaluate the wave attenuation efficiency of CT3N-WIP1 modular porous breakwaters.

5. Methods

To achieve the research objectives and address the study's content, the candidate employs the following main research methods: Literature review; Experimental research on physical models; Expert consultation; Applied research methodology.

6. Scientific and Practical Significance

Clarifying the interaction mechanism between waves and structures, and developing an empirical formula.

Providing a sustainable design solution that supports climate change adaptation and opens new directions for research and applications in hydraulic engineering and coastal environmental protection.

7. New contributions

- Elucidating the fundamental factors governing the process of wave transmission through modular porous breakwaters constructed with CT3N-WIP1 components.

- Developing a generalized empirical formula for calculating the wave transmission coefficient through the structure (Formula 3.10):

$$K_t = -0{,}30 \cdot min\left(0{,}75, \frac{R_c}{H_{m0,i}}\right) + 0{,}63\left(P_f \cdot \frac{B_f}{D}\right)^{-0{,}29}\left[1 - exp\left(-\frac{0{,}30}{\sqrt{s_{0m}}}\right)\right]$$

8. Thesis contents

In addition to the introduction and conclusion parts, the thesis consists of 3 chapter, as follows:

Chapter 1: Overview of Research on Breakwaters.

Chapter 2: Scientific Basis for the Research on Modular Porous Breakwaters Using CT3N-WIP1 Components.

Chapter 3: Results of Research on Wave Transmission Through Modular Porous Breakwaters Constructed with CT3N-WIP1 Components.

CHAPTER 1: OVERVIEW OF RESEARCH ON WAVE-REDUCING BREAKWATERS

1.1. General Introduction to Breakwaters

Definition: breakwaters are hydraulic structures designed to dissipate wave energy before it impacts the shoreline. WRBs can be constructed in seas, river mouths, or along coasts to protect shorelines, infrastructure, and ecosystems.

Key Features:

- Mechanism of Action: breakwaters dissipate wave energy through transmission, reflection, and scattering mechanisms.

- Classification: breakwaters are categorized based on: Structure: Submerged breakwaters, floating breakwaters, porous/hollow breakwaters. Material: Concrete, rubble mound, porous materials. Construction location: Nearshore or offshore.

1.2. Overview of Applications and Studies on Breakwaters

Globally: Countries like Japan, Italy, and the United States have implemented various WRB designs and materials, ranging from

submerged concrete and rubble mound breakwaters to porous structures like Reef Ball. Numerous studies focus on evaluating wave attenuation efficiency using physical experiments and numerical models, developing empirical formulas for calculating wave transmission coefficients. Major research programs such as DELOS (Europe) and LEACOAST2 (UK) have contributed significantly to understanding the interaction mechanisms between waves and WRBs.

In Vietnam: Common breakwaters types include rubble mound breakwaters, concrete breakwaters, and porous structures like Geotube, bamboo piles, and soft structures such as biological fences. Several solutions tested in the Mekong Delta, particularly in the West Sea of Ca Mau, have demonstrated high efficiency in wave attenuation and sediment deposition.

1.3. Overview of breakwaters solutions in the Mekong Delta

The Mekong Delta is significantly affected by coastal erosion and mangrove degradation. Wave-reducing solutions implemented in this region include: Porous breakwaters: Reduce wave energy, support sediment deposition, and restore mangroves; Environmentally friendly materials: Bamboo piles, wooden structures combined with mangrove plantation; Submerged and floating breakwaters: Combined with other coastal protection measures to enhance efficiency.

1.4. Conclusion of Chapter 1

This chapter summarizes and analyzes studies on breakwaters both domestically and internationally, clarifying research gaps in wave attenuation efficiency, particularly for modular porous/hollow structures. Investigating breakwaters constructed with CT3N-WIP1 components in the West Sea of Ca Mau is not only essential but also holds significant scientific and practical implications.

CHAPTER 2: SCIENTIFIC BASIS FOR THE RESEARCH ON MODULAR POROUS BREAKWATERS USING CT3N-WIP1 COMPONENTS

2.1. Introduction to the Study Area

The West Sea region is characterized by weak soil foundations, a gentle seabed slope, and complex hydrodynamic conditions, making it highly susceptible to coastal erosion. The severe degradation of mangrove forests further exacerbates erosion and land loss. This calls for effective wave attenuation solutions that can support sediment deposition and mangrove restoration.

2.2. Modular Porous breakwaters using CT3N-WIP1 components

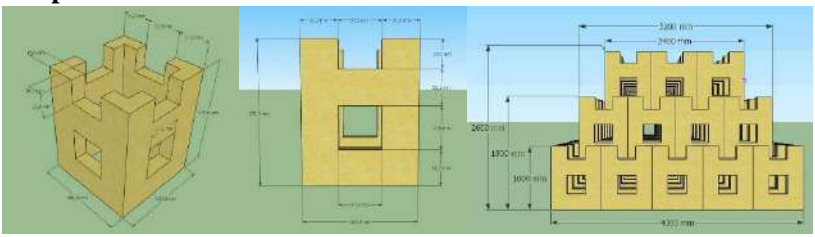

Figure 2-2. CT3N-WIP1 Components (CK1)

CT3N-WIP1 Components: A modular, porous, and hollow structure capable of dissipating wave energy and reducing wave reflection. Flexible in adjusting cross-sectional dimensions. Supports sediment deposition and creates favorable conditions for mangrove growth.

2.3. Wave Energy Balance

Neglecting the wave energy dissipation due to seabed friction and assuming that linear wave theory is sufficiently reliable to describe wave energy flux, the wave energy balance equation for wave-reducing breakwaters can be expressed as follows:

$$K_R^2 + K_t^2 + \varepsilon_D = 1 \quad (2.1)$$

2.4. Establishing the General Equation for Wave Transmission Coefficient

The dissertation applies the PI-Buckingham theorem to establish general equations that represent the relationship between fundamental influencing parameters, organized into dimensionless quantities, and the wave transmission coefficient K_t. The general equation determines the dimensionless quantity (Π) as follows:

$$\Pi = H_{mo,i}^{x1} . H_{mo,t}^{x2} . R_c^{x3} . B_f^{x4} . L^{x5} \quad (2.2)$$

Where x_1, x_2, x_3, x_4, x_5 are the exponents corresponding to the independent variables under consideration.

Table 2-1. Dimensional Analysis Matrix

Dimensional Analysis	**$H_{mo,i}$**	**$H_{mo,t}$**	**R_c**	**B_f**	**L**
[L]	1	1	1	1	1
[T]	0	0	0	0	0
[M]	0	0	0	0	0

Based on the dimensional analysis of the parameters, the dimensionless quantities Π_1, Π_2, Π_3, Π_4 are determined as follows:

- $\Pi_1 = H_{mo,i}^{-1} H_{mo,t}^{1} R_c^{0} B_f^{0} L^{0} = \frac{H_{mo,t}}{H_{mo,i}} = K_t$: Wave Transmission Coefficient
- $\Pi_2 = H_{mo,i}^{-1} H_{mo,t}^{0} R_c^{1} B_f^{0} L^{0} = \frac{R_c}{H_{mo,i}}$: Relative Submergence
- $\Pi_3 = H_{mo,i}^{-1} H_{mo,t}^{0} R_c^{0} B_f^{1} L^{0} = \frac{B_f}{H_{mo,i}}$: Relative Width
- $\Pi_4 = H_{mo,i}^{-1} H_{mo,t}^{0} R_c^{0} B_f^{0} L^{1} = \frac{L}{H_{mo,i}} \sim S_{om}^{-1}$: Wave Slope

Thus, the general Buckingham Π\PiΠ-theorem function can be expressed as follows:

$$K_t = \frac{H_{mo,t}}{H_{mo,i}} = f\left(\frac{R_c}{H_{mo,i}}, \frac{B_f}{H_{mo,i}}, s_{0m}\right) \quad (2.5)$$

Additionally, the permeability parameter of the breakwaters also affects the wave attenuation efficiency. When combined with the average width of the WRB, the general formula can be expressed as follows:

$$K_t = \frac{Hmo,t}{Hmo,i} = f(\frac{Rc}{Hmo,i}, Pf\frac{Bf}{Hmo,i}, s_{0m}) \quad (2.6)$$

This serves as the basis for determining the parameters to be measured in the design of physical model experiments in the wave flume.

2.5. Research Methods Using Physical Models

The physical model was chosen with a scale ratio of $\lambda_L = \lambda_h =$ 8, The time scale ratio λ_t (including wave periods) was determined according to the length scale under Froude's standard criteria.

Table 2-3. Parameters and Scale Relations

Quantities	**Relation**	**Prototype-to-Model Scale**
Length and Height (m)	$\lambda_L = \lambda_h$	8
Time and Period (s)	$\lambda_t = \sqrt{\lambda_L}$	2,83

The wave flume has an effective length of 43 m, a width of 1.0 m, and a height of 1.2 m. It is equipped with an Active Reflection Compensation (ARC) system to eliminate reflected wave interference from the wave generator. The wave generator can produce random waves according to specific spectra (JONSWAP, TMA, PM), with a maximum random wave height of 0.3 m and a maximum wave period of 3 seconds. Capacitance-based wave gauges with high accuracy (± 0.1 mm) and a sampling frequency of up to 100 Hz were used to measure water surface fluctuations. A three-dimensional velocity meter (Vectrino-II), operating on the principle of optical backscatter, was employed to measure flow velocity.

b) Experimental Setup

The experimental layout is shown in Figure 2.3. The forest bed model was constructed using smooth cement mortar, with a height of 0.5 m. The flat bed section is 10 m long with a slope i = 1/500, The transition section is 10 m long with a slope i = 1/20. The WRB model in the wave flume was scaled down according to the model dimensions in Table 2-3. Five wave gauges (labeled WG) were used to measure wave variations in front of the forest bed, and before and after the WRB. The wave attenuation efficiency of the WRB was evaluated using wave height measurements before (WG4) and after (WG5) the structure. The three-dimensional velocity meter (Vectrino-II), synchronized with WG4, was used to analyze reflected waves from the structure under shallow water conditions (nonlinear waves) based on the method by Sheremet et al. (2002).

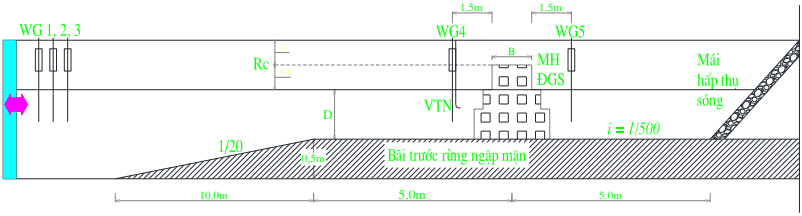

Figure 2-3. Experimental Layout

Figure 2-4. Physical model

Table 2-4. Parameters of breakwater in physical model

Model	Width B (m)	Height H (m)	Porosity n (-)	Notes
CT3N-WIP1 Components	0,2 ÷ 0,3	0,30	0,60 ÷ 0,70	

c) Measurement Parameters

Significant wave height H_{m0}:

$$H_{m0} = 4{,}004\ \sqrt{m_0} = 4{,}004\ \sqrt{\int_{f\min}^{f\max} S(f)df} \tag{2.7}$$

Spectral peak period T_p, and mean wave period $T_{m-1,0}$:

$$T_p = \frac{1}{f_p} \tag{2.8}$$

$$T_{m-1,0} = \frac{m_{-1}}{m_0} = \frac{\int_{f\min}^{f\max} f^{-1}S(f)df}{\int_{f\min}^{f\max} S(f)df} \tag{2.9}$$

Wave lengths in deep water L_0 and shallow water L at depth d:

$$L_{0p} = \frac{g}{2\pi}T_p^2 \tag{2.11}$$

$$L_{0m} = \frac{g}{2\pi}T_m^2 \tag{2.12}$$

$$L_p = L_{0p}\ tanh\left(\frac{2\pi}{L_{0p}}D\right) \tag{2.13}$$

$$L_m = L_{0m}\ tanh\left(\frac{2\pi}{L_{0m}}D\right) \tag{2.14}$$

The combined wave reflection coefficient was determined from the ratio of reflected wave flux to incoming wave flux.

$$K_R^2 = \frac{F^-}{F^+} \tag{2.15}$$

Wave flux values were calculated from synchronized wave and flow measurements taken at the position before the WRB:

$$F^{\pm} = \frac{1}{4}\sqrt{gh}\left[C_{o\eta\eta}(f) \pm (2\sqrt{h/g})C_{o\eta u}(f) + (h/g)C_{ouu}(f)\right] \tag{2.16}$$

Experimental scenarios for the breakwaters model were designed from 12 wave parameter combinations, including: Six wave heights H_{m0} ranging from 0.07 m to 0.18 m (equivalent to 0.5 m to 1.50 m in real conditions). Two representative monsoon wave slopes s_{0p} = 0,02 and 0,035, three water levels. Waves generated at the deep-water boundary followed the standard JONSWAP spectrum.

Table 2-5. Summary of Wave Testing Scenarios

Water Depth D (m)	**Prototype Hydrodynamic Conditions**		**Model Hydrodynamic Conditions**		**Notes**
	H_{m0} (m)	**T_p (s)**	**H_{m0} (m)**	**T_p (s)**	
0,20 0,30 0,40	0,56	3,20	0,07	1,13	- Model scale $\lambda_L = \lambda_h = 8$; - Froude's standard; - 12 Wave Scenarios; - 03 Water Depths.
	0,56	4,25	0,07	1,50	
	0,8	5,09	0,10	1,80	
	0,8	3,82	0,10	1,35	
	0,96	5,66	0,12	2,00	
	0,96	4,25	0,12	1,50	
	1,12	5,94	0,14	2,10	
	1,12	4,53	0,14	1,60	
	1,28	6,51	0,16	2,30	
	1,28	4,81	0,16	1,70	
	1,44	6,79	0,18	2,40	
	1,44	5,09	0,18	1,80	

Scenarios included variations in the geometry, porosity, and arrangement of CT3N-WIP1 components. A total of 348 tests were conducted, accounting for monsoon wave characteristics in the West Sea of Ca Mau to comprehensively evaluate the effects of key influencing parameters on wave transmission.

Experiment Procedure:

- Build the model, fabricate CT3N-WIP1 components, inspect, and install measurement equipment.

- Calibrate and validate the model.

- Conduct scenarios without the structure.

- Conduct scenarios with the structure, varying the porosity of CT3N-WIP1 components.

2.5. Conclusion of Chapter 2

Chapter 2 has established a solid scientific foundation for studying the wave attenuation efficiency of modular porous breakwaters constructed with CT3N-WIP1 components. Influencing factors, experimental methods, and the basis for developing empirical formulas have been clearly presented, forming the groundwork for future research.

CHAPTER 3: RESULTS OF RESEARCH ON WAVE TRANSMISSION THROUGH MODULAR POROUS BREAKWATERS CONSTRUCTED WITH CT3N-WIP1 COMPONENTS

3.1. Wave transmission coefficient through CT3N-WIP1 components

The wave transmission coefficient is influenced not only by the porous nature of the dike body but also by its geometric dimensions (height, width).

The analysis begins by assessing the impact of parameters influencing wave transmission through the breakwaters.

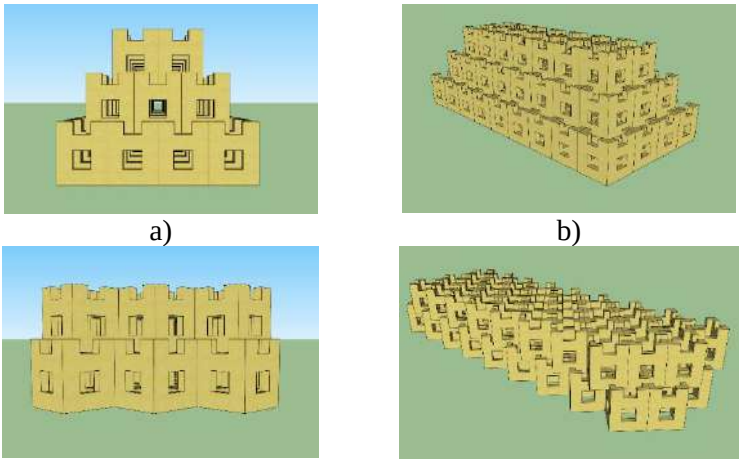

a) b)

c) d)

Figure 3-1. Two Arrangement Options for CT3N-WIP1 Components (a), b): Straight; c), d): staggered 45°

3.1.1. Influence of Width

The crest width B is a critical parameter affecting K_t and has an inverse relationship with it. The analysis of the relative crest width (B/H_{m0} and B/D) is shown in Figure 3.2, corresponding to different crest freeboard heights (R_c) Results indicate that the relationships ($K_t \sim B/H_{m0}$) and ($K_t \sim B/D$) are inversely proportional and nonlinear, especially pronounced when R_c is large (R_c = 0,08m ÷ 0,18m).

The figure demonstrates that, under the same submergence conditions, the relative width of the breakwaters has a significant impact on $K_t$showing a stronger inverse relationship when the freeboard height is large.

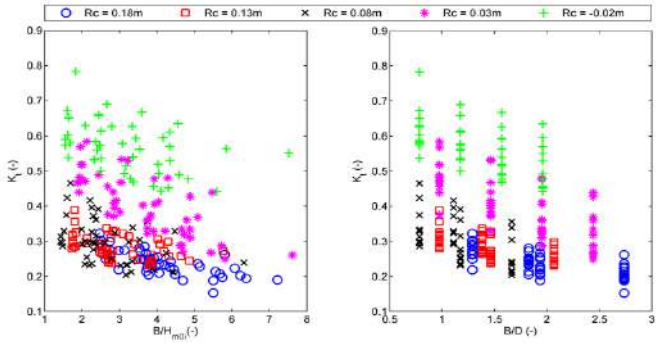

Figure 3-2. Influence of relative crest width B/H_{m0} and B/D

3.1.2. Influence of Crest Submergence

Crest submergence refers to the distance from the water surface to the crest of the breakwaters.

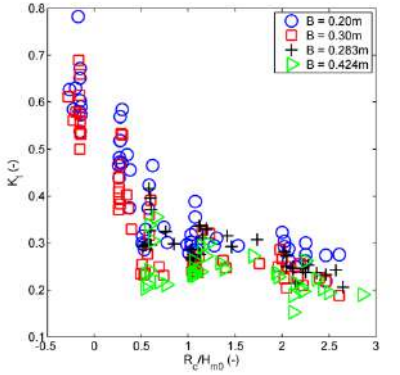

Figure 3-3. Influence of Crest Submergence $K_t \sim R_c/H_{m0i}$

The relationship ($K_t \sim R_c/H_{m0}$) exhibits a clear inverse trend. K_t decreases rapidly as R_c/H_{m0} increases up to a threshold $R_c/H_{m0} \leq (0{,}75 \div 1{,}0)$. When the crest height exceeds the water level, $R_c/H_{m0} > (0{,}75 \div 1{,}0)$, K_t decreases more slowly and becomes less dependent on R_c/H_{m0} as wave transmission occurs primarily through the porous dike body.

3.1.3. Influence of Wave Period

This study uses the spectral mean wave period $T_{m\text{-}1,0}$, which emphasizes the role of long wave components in shallow water conditions.

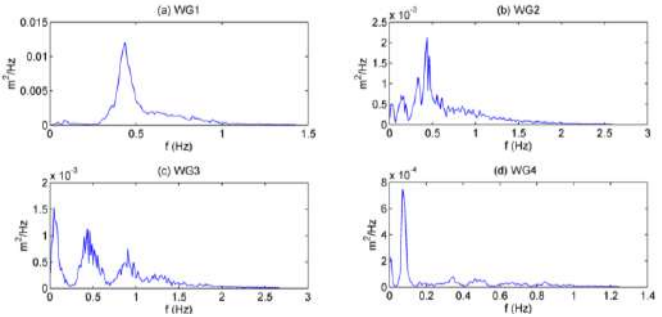

Figure 3-4. Wave Period

Generally, K_t exhibits an inverse relationship with the wave slope s_{0m}, meaning a direct relationship with $T_{m\text{-}1,0}$ (longer waves result in higher wave transmission). This dependency becomes more pronounced for elevated crests (R_c lớn, $R_c \geq 0{,}03$m in Figure 3.5).

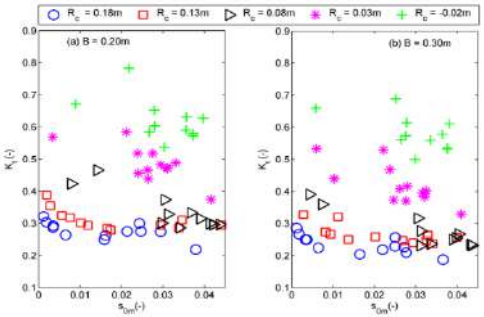

Figure 3-5. Influence of Wave Period

3.1.4. Influence of Porosity

The porosity of the dike or its armor layers significantly affects wave-structure interaction, directly influencing the wave energy balance through the structure.

In this study, the impact of porosity is analyzed using CT3N-WIP1 components with varying configurations of pore openings on four sides. Two cases are examined n = 62% (CK1) and n = 66% (CK2).

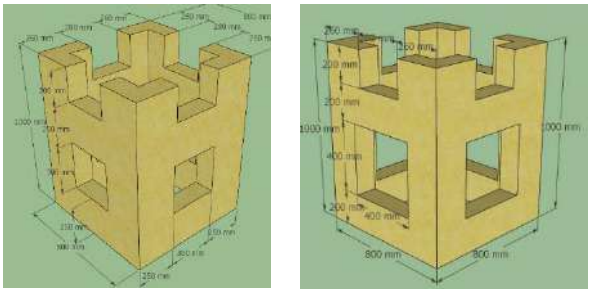

(a) (b)

Figure 3-6. Components CK1 (a) và CK2 (b)

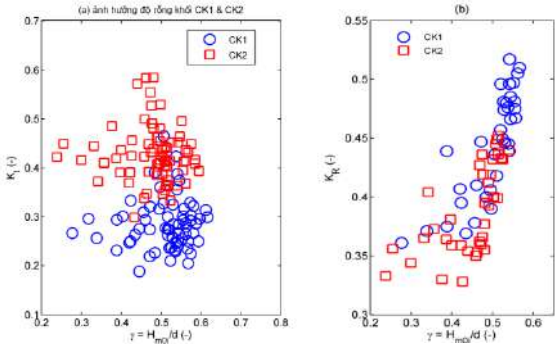

Figure 3-7. Effect of Porosity on Wave Transmission Coefficient and Reflection Coefficient Between CK1 and CK2

3.2. Wave Reflection

Wave reflection is a key indicator of wave-structure interaction, critical for evaluating structures supporting mangrove restoration. The reflection coefficient K_R is essential for determining incident and transmitted wave heights ($H_{s,i}$ và $H_{s,t}$), used to calculate K_t based on wave energy balance equations:

$$H_{s,i} = \frac{H_{s,t}}{\sqrt{1+K_R^2}} \tag{3.1}$$

Using synchronous wave and flow measurements, K_R is determined via Sheremet et al. (2002). For elevated crests, follows an exponential trend with wave breaking indices γ as commonly observed for marine structures:

$$K_R = a \cdot exp(b \cdot \gamma) \tag{3.3}$$

Based on the results of the experimental regression analysis (see Figure 3-9a), the equation (3.3) for the case of elevated breakwaters can be rewritten as follows:

$$K_R = 0{,}24 \cdot exp(1{,}22 \cdot \gamma) \tag{3.4}$$

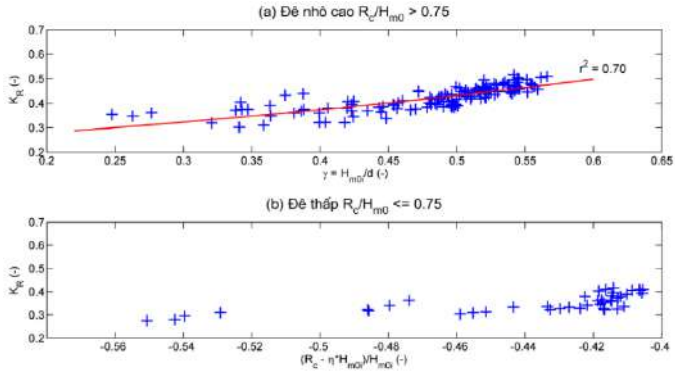

Figure 3-9. Wave Reflection: (a) High-crest dike R_c/H_{m0} >0,75 (b) Low-crest dike $R_c/H_{m0} \leq 0{,}75$

Equation (3.4) indicates that when the wave height is small relative to the water depth, the reflection coefficient approaches a limiting value of K_R = 0,24.

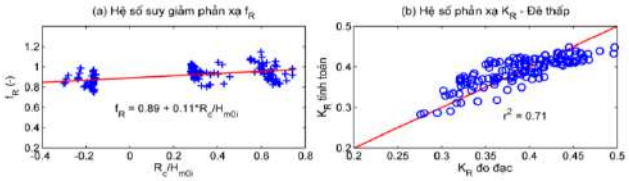

Figure 3-10. $R_c/H_{m0} \leq 0{,}50$: (a) Reflection Reduction Factor f_R; (b) Comparison of Reflection Coefficients

For the case of low-crest or submerged breakwaters, the reflection coefficient is still determined using Formula . (3.4) but is adjusted with a reduction factor to account for the influence of the low crest (see Figure 3-10a):

$$K_R^L = f_R \cdot K_R = 0{,}24 \cdot exp(1{,}22 \cdot \gamma) \cdot f_R \quad (3.5)$$

$$f_R = 0{,}89 + 0{,}11 \cdot \frac{R_c}{H_{m0i}} \quad (3.6)$$

In Equation (3.6), the freeboard height R_c can take negative values, corresponding to cases where the dike crest is submerged below the calculated water level. It is observed that for low-crest breakwaters, wave reflection decreases compared to high-crest breakwaters and follows a linear trend with the relative freeboard height R_c/H_{m0i}. When $R_c/H_{m0i} = 0{,}75$ the reflection reduction factor $f_R \approx 1{,}0$.

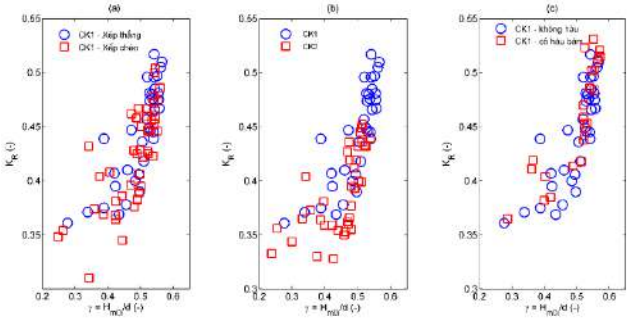

Figure 3-11. Comparison of Reflection Coefficients: (a) Change in Arrangement (b) Change in Porosity (c) Presence of Biofouling

When comparing the reflection coefficient between straight and staggered arrangements (using the same CK1 component, Figure 3-11a) and between two component types with different porosities (CK1 and CK2 in straight arrangements, Figure 3-11b) under identical hydraulic conditions (refer to Appendix A for dike model arrangement scenarios), it is observed that: Rotating the components by 45° increases turbulence and the volumetric porosity of the dike body, leading to enhanced wave absorption and, consequently, a lower reflection coefficient compared to the straight arrangement. A significant difference in reflection coefficients is noted between the two cases. The CK2 component, with larger side openings, results in greater porosity of the dike body. This leads to a higher proportion of wave energy transmitted through the porous dike body, thereby significantly reducing the reflection coefficient compared to the CK1 component. However, due to structural and practical requirements, the CK2 component's thin-walled design may compromise its structural stability (e.g., cracking or breaking) during real-world applications. For this reason, detailed studies on CK2 are not pursued at this stage. The experimental data presented in this report primarily involve tests with CK1 components. Over time, when biofouling (e.g., oyster attachment) occurs on the dike body, the reflection coefficient is expected to increase slightly compared to its initial state without biofouling (for CK1 arrangements). However, this difference is negligible.

3.3. Results of Wave Transmission Calculation Methodology

General Formula:

$$K_t = a_1 \cdot \min\left(\eta, \frac{R_C}{H_{m0i}}\right) + a_2 \left(P_f \cdot \frac{B_f}{D}\right)^{c_1} \left[1 - \exp\left(\frac{c_2}{\sqrt{s_{0m}}}\right)\right] \quad (3.7)$$

Regression analysis identifies the coefficients a_1 = –0,30 and a_2 = 0,63, with corresponding c_1 = - 0,29 và c_2 = - 0,30, yielding the highest correlation coefficient (r^2 = 0,89).

The final general formula is expressed as:

$$K_t = -0{,}30 \cdot min\left(0{,}75, \frac{R_c}{H_{m0,i}}\right) + 0{,}63 \left(P_f \cdot \frac{B_f}{D}\right)^{-0{,}29} \left[1 - exp\left(-\frac{0{,}30}{\sqrt{s_{0m}}}\right)\right] \quad (3.10)$$

The formula, based on CK1 block arrangements (straight and staggered), demonstrates high reliability when validated against experimental data, as shown in Figure 3.15. Adjusting for staggered arrangements through an effective width increase further enhances its accuracy.

Using the formula to calculate K_t for breakwaters with different porosities confirms its general applicability. Experimental results indicate that staggered arrangements increase turbulence and absorption, reducing wave reflection coefficients.

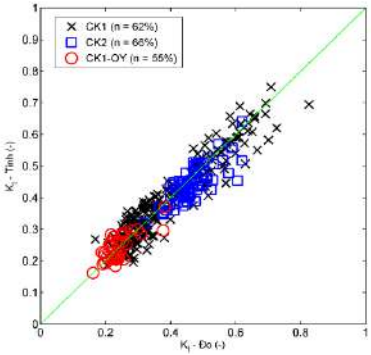

Figure 3-15. Comparison of Wave Transmission Coefficients Based on Porosity Changes

3.4. Application of Research Results in Cross-Section Design Testing

The empirical formula (3.10) developed is in a dimensionless form. The application range of these formulas corresponds to the relative variation of influencing parameters in the physical model experiments.

Table 3-1. Application Scope of the Empirical Formula

Parameter	Range	Notes
Deep-water wave height $H_{m0,0}$ (m)	0,7 ÷ 2,0	Characterizes monsoon waves approaching the structure
Deep-water wave period T_p (s)	3,0 ÷ 7,0	
Wave height before the structure H_{m0i} (m)	0,50 ÷ 1,50	
Wave slope s_{0p} (-)	0,019 ÷ 0,053	
Relative crest submergence R_c/H_{m0} (-)	–0,30 ÷ 3,10	Represents the geometric characteristics of the structure
Wave breaking index $\gamma = H_{m0i}/D$ (-)	0,24 ÷ 0,64	
Relative crest width B/D (-)	0,80 ÷ 2,70	
Relative crest width B/H_{m0} (-)	1,37 ÷ 7,60	
Number of rows on crest (width)	≥ 2	Structural configuration of the dike
Number of stacked rows (height)	≥ 2	
Block arrangement style	Straight, staggered 45°	
Porosity of the breakwaters n (-)	0,55 ÷ 0,66	

For shallow water depths, two options for crest height can be selected:

- High-crest dike with three stacked rows (2.60 m).
- Low-crest dike with two stacked rows (1.80 m).

The dike width is then determined based on the wave reduction requirement behind the dike, for example, $H_{m0,t} \leq 0{,}30$m m or the allowable wave transmission coefficient $[K_t] \leq 0{,}35$. To facilitate the selection of dike width under different conditions, a relationship diagram between the wave transmission coefficient and average dike width ($K_t \sim B_f$) is constructed.

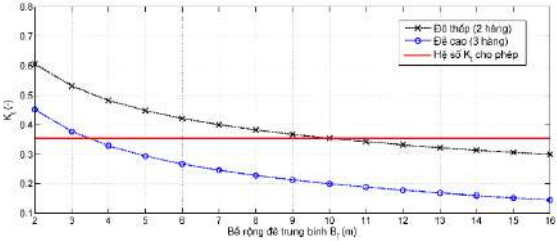

Figure 3-17. The results of the relationship ($K_t \sim B_f$) for the cases of high-crest and low-crest breakwaters

The results from the relationship diagram ($K_t \sim B_f$), shown in Figure 3-17, indicate the following:

- To meet wave reduction requirements: For high-crest breakwaters, the average dike width must be $B_f \geq 3{,}5$m. For low-crest breakwaters, $B_f \geq 10$m.

- Correspondingly, the following configurations can be chosen: High-crest dike: Four straight rows on the crest ($B = 3{,}2$m, $B_f = 4{,}0$m). Low-crest dike: Thirteen straight rows on the crest ($B = 10{,}4$m, $B_f = 10{,}8$ m).

- For staggered arrangements with a 45° rotation, $b = 0{,}80 \times \sqrt{2} = 1{,}13$m, leading to: $B \geq 2{,}37$m for high-crest breakwaters. $B \geq 9{,}44$m for low-crest breakwaters.

Correspondingly: High-crest dike: Three staggered rows on the crest (B = 3,39m và B_f = 4,52m). Low-crest dike: Nine staggered rows on the crest (B = 10,17m và B_f = 10,74m).

(a) (b)

Figure 3-18. cross-sectional design of High-crest breakwaters (a) and Low-crest breakwaters (b)

3.5. Conclusion of Chapter 3

Chapter 3 clarified the wave transmission mechanism through CT3N-WIP1 components using physical experiments and empirical formulas. The research results achieved the following:

- Confirmed the high wave attenuation efficiency of modular breakwaters constructed with CT3N-WIP1 components.

- Provided scientific tools for calculations and designs, enabling effective practical applications.

- Proposed cross-sectional design solutions that meet the needs of coastal protection and mangrove restoration in the West Sea of Ca Mau.

The content of Chapter 3 elucidated the mechanism and wave attenuation efficiency of CT3N-WIP1 modular breakwaters and offered calculation tools and cross-sectional design options suitable for practical applications. The research results not only fulfilled the dissertation's objectives but also provided a scientific foundation for the design and implementation of breakwaters in coastal regions with similar conditions.

CONCLUSIONS AND RECOMMENDATIONS

1. The obtained results

The thesis has completed the research objectives and achieved the following outstanding results: (1) The dissertation synthesized domestic and international studies, clarifying the factors influencing the wave transmission process through modular breakwaters constructed with CT3N-WIP1 components. (2) Established the scientific basis for modular breakwaters constructed with CT3N-WIP1 components. (3) Developed an empirical formula for calculating the wave attenuation efficiency of modular breakwaters constructed with CT3N-WIP1 components. (4) Analyzed trends and the extent of influence of key governing parameters. (5) Proposed design alternatives for cross-sections of modular breakwaters constructed with CT3N-WIP1 components. (6) The research results provide a scientific foundation and calculation tools for evaluating the wave attenuation efficiency of modular porous breakwaters in coastal areas of Vietnam.

2. New constributions

- Elucidating the fundamental factors governing the process of wave transmission through modular porous breakwaters constructed with CT3N-WIP1 components.

- Developing a generalized empirical formula for calculating the wave transmission coefficient through the structure (Formula 3.10):

$$K_t = -0{,}30 \cdot min\left(0{,}75, \frac{R_c}{H_{m0,i}}\right) + 0{,}63\left(P_f \cdot \frac{B_f}{D}\right)^{-0{,}29}\left[1 - exp\left(-\frac{0{,}30}{\sqrt{s_{0m}}}\right)\right]$$

3. Limitations, recommendations and future research

- Limitations: The results only reflect the wave-structure interaction process and do not comprehensively assess the long-term stability of modular breakwaters constructed with CT3N-WIP1 components. The applicability of the results to other regions with different hydrodynamic and geological conditions has not been evaluated.

- Future Directions: Assessing the impact of bivalve organisms on the wave attenuation efficiency and sediment exchange capacity of modular breakwaters constructed with CT3N-WIP1 components. Conducting field experiments to validate findings. Integrating physical modeling with numerical modeling. Researching and proposing optimal dimensions and configurations for modular WRBs constructed with CT3N-WIP1 components.

4. Recommendations

(1) Incorporate the new contributions of the dissertation into reference materials for designing breakwaters structures in Vietnam. (2) Pilot the application of modular breakwaters constructed with CT3N-WIP1 components in the coastal mudflat area of the West Sea of Ca Mau.

LIST OF PUBLISHED PAPERS

1. Mai Trong Luan, Thieu Quang Tuan (2023), "Physical model evaluation of the effectiveness of several types of wave-reducing dike structures," *Journal of Water Science and Technology*, 81, pp. 2–7.
2. Mai Trong Luan, Tran Dang Trung (2023), "Assessment of vulnerability in the Ca Mau coastal area as a basis for identifying nature-based coastal protection solutions," *Journal of Water Science and Technology*, 76, pp. 34–53.
3. Thieu Quang Tuan, Mai Trong Luan, Le Ngoc Cuong (2022), "Laboratory study of wave damping by porous breakwaters on mangrove mudflats in the Mekong River Delta", *Ocean Engineering*, 258 (2022).
4. Mai Trong Luan, Nguyen Quoc Huy, Mac Van Dan (2021), "Cyclic patterns in erosion and accretion processes along the western coastline of Ca Mau Province," *Journal of Water Resources*, 2(2021), pp. 39–47.
5. Trinh Quang Toan, Nguyen Van Tuan, Mai trong Luan, Mac Van Dan, Nguyen Ngoc (2021), "Changes in Wave Spectrum Under Impact of the Breakwater Construction over the West Sea in Ca Mau Vietnam", 2021 *4th International Conference on Mechanical Manufacturing and Industrial Engineering*, pp.46-50.
6. Thieu Quang Tuan, Mai Trong Luan (2020), "Monsoon wave transmission at bamboo fences protecting mangroves in the lower mekong delta", *Applied Ocean Research*, 2020.
7. Mai Trong Luan, Nguyen Quoc Huy (2019), "Evaluation of coastal protection solutions applied in the eastern coast of the Ca Mau Peninsula," *Scientific and Technological Compilation:*

Celebrating 60 Years of Development of the Vietnam Institute of Water Resources Science (2014–2019), pp. 694–703.